Influence of SBS on the Aging Properties of High-Content Terminal Blend Rubber Modified Asphalt

Wang, Sheng; Huang, Weidong; Liu, Xueyan; Lin, Peng

DOI
10.1061/JMCEE7.MTENG-15506

Publication date
2023

Document Version
Final published version

Published in
Journal of Materials in Civil Engineering

Citation (APA)
Wang, S., Huang, W., Liu, X., & Lin, P. (2023). Influence of SBS on the Aging Properties of High-Content Terminal Blend Rubber Modified Asphalt. *Journal of Materials in Civil Engineering*, *35*(8), Article 04023260. https://doi.org/10.1061/JMCEE7.MTENG-15506

Influence of SBS on the Aging Properties of High-Content Terminal Blend Rubber Modified Asphalt

Sheng Wang[1]; Weidong Huang[2]; Xueyan Liu[3]; and Peng Lin[4]

Abstract: The goal of this study was to investigate the effect of styrene-butadiene-styrene (SBS) polymer on the aging properties of high-content terminal blend rubber modified asphalt (HCTBMA). All asphalt was tested for chemo-rheological properties using an attenuated total reflection–Fourier transform infrared spectroscopy (ATR-FTIR) test, temperature sweep test, frequency sweep tests, and multiple stress creep recovery (MSCR) test. According to ATR-FTIR observations, SBS can retard the oxidation effect of HCTBMA during short-term aging, but its inhibitory effect is reduced during long-term aging. Furthermore, aging aggravates the degree of desulfurization of crumb rubber in HCTBMA as the SBS content increases. Compared with HCTBMA, neat asphalt has a lower elasticity at high temperatures and a higher elasticity at low temperatures. The addition of SBS to HCTBMA improves the elasticity of the material. The elasticity of HCTBMA decreases and then increases after aging, and SBS can reduce the aging degree of HCTBMA after aging. Moreover, based on Pearson correlation analysis, the correlation between the desulfurization of rubber and the degradation of polybutadiene in HCTBMA during aging is high. **DOI: 10.1061/JMCEE7.MTENG-15506.**

Author keywords: High-content terminal blend rubber modified asphalt (HCTBMA); Chemo-rheological properties; Aging properties; Oxidation effect; Pearson correlation.

Introduction

Rubber modified asphalt (RMA) with excellent properties of high temperature, aging resistance, and fatigue resistance can be obtained by processing waste tires into crumb rubber (CR) and modifying neat asphalt (Bressi et al. 2019; Picado-Santos et al. 2020; Lo Presti 2013; Sienkiewicz et al. 2017; Wang et al. 2017). The use of RMA in road pavement construction can not only save the amount of neat asphalt but also consume a large number of waste tires, which is of great significance to environmental protection (Shen et al. 2017). Scholars have investigated the performance of RMA (Bressi et al. 2019; Picado-Santos et al. 2020; Lo Presti 2013; Sienkiewicz et al. 2017). Wang et al. (2012) investigated the low-temperature performance of RMA with CR content of 10%, 15%, 20%, and 25%, respectively, and discovered that increasing the CR content improved the low-temperature performance of RMA, but the difference in low-temperature performance between the CR content of 20% and 25% was not significant. Dong et al. (2011) evaluated a pre-desulfurized RMA with a content level of 25% and found that the pre-desulfurized RMA had excellent fatigue performance compared with conventional RMA. However, due to the lack of sufficient chemical interaction between CR and asphalt, most CR exists in asphalt in the form of swelling, forming a solid-liquid two-phase system, resulting in poor RMA storage stability and thus limiting the amount of CR (Han et al. 2016).

The terminal blend (TB) process is a preparation method that can increase the CR content in RMA (Wang et al. 2021c, 2022a). Under high temperatures and long-time mixing conditions, terminal blend rubberized asphalt (TBRA) is carried out with CR and neat asphalt, thus allowing full desulfurization and degradation of CR (Wang and Huang 2021). Compared with RMA produced by conventional processes, TBRA has the advantages of high stability, excellent low-temperature ductility, high fatigue, and less susceptibility to segregation (Jones et al. 2008; Qi et al. 2006; Santucci 2009). Nazzal et al. (2017) studied TBRA and found that the mixing speed of TBRA affects its properties and that TBRA had better indirect tensile strength, water damage resistance, low-temperature crack resistance, and rutting resistance. Lo Presti et al. (2012) tested the influence of CR particle size, doping, and processing temperature and found that the rate of desulfurization of TBRA increased with increasing temperature, but that excessive temperatures caused the aging of TBRA. The workability of TBRA has been greatly improved, which can well meet engineering needs. However, the long chains of CR are broken during the desulfurization process and its relative molecular mass is significantly reduced, resulting in a decrease in the TBRA's high-temperature property (Abdelrahman 2006). The results of the previous studies indicate that the high-temperature performance of RMA under the TB process is poor, and to achieve the TB process with RMA technology, other modifiers need to be compounded to improve the indicators. One of the most used modifiers in engineering is styrene-butadiene-styrene (SBS), and studies have shown that SBS can improve the high-temperature performance of RMA without significantly affecting other properties of TBRA (Lin et al. 2017; Tang et al. 2018). The formation of a network structure of CR

[1]Ph.D. Candidate, Key Laboratory of Road and Traffic Engineering of Ministry of Education, Tongji Univ., Tongda Bldg., 4800 Cao'an Rd., Shanghai 201804, China (corresponding author). ORCID: https://orcid.org/0000-0001-9784-0150. Email: shengwang985@163.com

[2]Professor, Key Laboratory of Road and Traffic Engineering of Ministry of Education, Tongji Univ., Tongda Bldg., 4800 Cao'an Rd., Shanghai 201804, China. Email: hwd@tongji.edu.cn

[3]Associate Professor, Section of Pavement Engineering, Dept. of Engineering Structures, Faculty of Civil Engineering and Geosciences, Delft Univ. of Technology, Stevinweg 1, Delft 2628 CN, Netherlands. Email: X.Liu@tudelft.nl

[4]Postdoctoral Researcher, Section of Pavement Engineering, Dept. of Engineering Structures, Faculty of Civil Engineering and Geosciences, Delft Univ. of Technology, Stevinweg 1, Delft 2628 CN, Netherlands. Email: p.lin-2@tudelft.nl

Note. This manuscript was submitted on August 28, 2022; approved on January 23, 2023; published online on May 31, 2023. Discussion period open until October 31, 2023; separate discussions must be submitted for individual papers. This paper is part of the ***Journal of Materials in Civil Engineering***, © ASCE, ISSN 0899-1561.

and SBS in asphalt improves TBRA's high-temperature performance. However, both TBRA and SBS composite-modified asphalt require higher temperatures than pure asphalt during production and paving and are therefore more affected by oxidation (Li et al. 2021; Liu et al. 2020). Moreover, during the use of modified asphalt pavements, the asphalt often undergoes aging reactions and becomes brittle and hard due to the action of oxygen and sunlight (Xing et al. 2022), which in turn affects the performance of asphalt pavements and is susceptible to cracking under traffic loads and temperature stresses. Therefore, the aging performance of modified asphalt materials is of great concern. In previous studies, the content of CR in TBRA and SBS composite-modified asphalt was less than 20% (Apeagyei 2011; Arega et al. 2011; Asli et al. 2012; Safari et al. 2014; Stimilli et al. 2014). There are few studies on different contents of RMA prepared by the TB process with SBS (Al-Mansob et al. 2022; Al-Sabaeei et al. 2022), and the research on the aging behavior of high-content terminal blend rubber modified asphalt (HCTBMA) with SBS is not comprehensive.

In this paper, the effect of SBS on the aging properties of different contents of RMA prepared by the TB process was investigated. The chemical composition and rheological properties of TBRA with SBS were analyzed using the attenuated total reflection–Fourier transform infrared spectroscopy (ATR-FTIR) test, temperature sweep (TS) test, frequency sweep tests, and multiple stress creep recovery (MSCR) test before and after aging, respectively. The aging resistance of TBRA with SBS was assessed by the rheological indexes. In addition, correlations between chemical and rheological indexes of different contents of RMA prepared by the TB process were studied.

Material and Methods

Materials

In this paper, neat asphalt (PG 64-16) supplied by ESSO asphalt company (Exxon Mobil Corporation, Olathe, Kanas) and CR (40% of the HCTBMA weight) were used to produce HCTBMA. The RMA with 20% CR content was prepared to compare the performance of the HCTBMA. The HCTBMA and the RMA with 20% CR content were prepared by the TB process, referring to Wang and Huang (2021). The high-speed shear rate for the TB process in this trial was 6,000 rpm and because the modified binder was prepared in an oxygen-sealed vessel, the aging degree of the modified binder is very low. CR (30 mesh) was produced in Jiangyin, China, containing 54% natural rubber and synthesis rubber. The calculated ratio (3%, 5%) of linear SBS by weight of RMA and the RMA (20% and 40% by weight CR) was selected to prepare the binders by adding 3% by weight SBS and 5% by weight SBS to RMA for 60 min at 180°C, respectively. The SBS has a molecule weight of 120,000 g/mol. The details of the composition of RMA containing different contents of CR and SBS are given in Table 1.

Table 1. Composition of RMA containing different contents of CR and SBS

	Modification plan	
Sample	CR (%)	SBS polymer (%)
Neat_E	0	0
20TB_3SBS	20	3
20TB_5SBS	20	5
40TB_3SBS	40	3
40TB_5SBS	40	5

Aging Procedures

Rolling thin-film oven test (RTFOT) aging and pressure aging vessel (PAV) were carried out on the RMA containing different contents of CR and SBS according to JTG E20-2011 (Ministry of Transport of the People's Republic of China 2011), respectively.

ATR-FTIR Test

In this paper, the chemical structures of the RMA containing different contents of CR and SBS before and after aging were tested employing ATR-FTIR (Wang et al. 2021a, b). The spectra were collected for 32 scans in the wavenumber range 4,000–600 cm^{-1}. The aging process of asphalt results in the production of carbonyl groups. Therefore, the carbonyl index (I_{CA}) was chosen in this study to assess the degree of oxidation of the RMA containing different contents of CR and SBS (Wang et al. 2020). The desulfurization of the CR occurs during the aging process (Wang et al. 2022b; Wang and Huang 2021), resulting in the destruction of the original cross-linked structure of the CR, which allows a large amount of silica from CR to enter the asphalt, resulting in an increase in the silica index ($I_{Si-O-Si}$) of the asphalt. In this paper, silica index ($I_{Si-O-Si}$) and polybutadiene index (I_{PB}) were chosen to analyze the level of desulfurization of CR from RMA prepared by the TB process and the degradation of polybutadiene from RMA prepared by the TB process during aging.

The five infrared reference peak indexes commonly used in the aging evaluation of HCTBMA are shown in Fig. 1. In the study of aging, the reference peaks are selected to be less affected by aging. The reference peak area was taken as the stable methyl umbrella vibration at 1,376 cm^{-1}. Table 2 provides the I_{CA}, $I_{Si-O-Si}$, and I_{PB} calculation methods.

Measurements of Rheological Properties

TS tests were performed on the RMA containing different contents of CR and SBS before and after aging using a dynamic shear rheometer (DSR) to obtain the complex modulus (G^*) and phase angle (δ) in the range of 34°C to 88°C.

Master curves for G^*, δ, storage modulus (G'), and loss modulus (G'') were constructed on the RMA containing different contents of CR and SBS before and after aging from frequency sweep tests in the 5°C to 75°C range with a temperature increment of 10°C. The test frequencies ranged between 0.1 and 30 Hz. Based on the test results of the frequency sweep, the master curves of G^*, δ, G', and G'' were constructed using the sigmoidal model with the time-temperature superposition principle (TTSP) and 25°C as the reference temperature (which is representative of the service life of asphalt pavements), and the shift factors were automatically adjusted according to the model to obtain the best fit. The rheological master curves can correspond to the stress–strain response of the asphalt at different loading frequencies and different loading temperatures, thus simulating the asphalt rheological behaviors data over a large time (frequency) interval in a short test time.

According to AASHTO M 332-14 (AASHTO 2014), the MSCR tests were performed on the RMA containing different contents of CR and SBS before and after aging (unaged condition, RTFOT aging, PAV aging) from 64°C to 82°C with a temperature increment of 6°C to study the influence of aging on the rheological index of the MSCR test. Parallel plates with a diameter of 25 mm (gap of 1 mm) were used for measurements above 30°C and parallel plates with a diameter of 8 mm (gap of 2 mm) were used for tests below 30°C for these tests on DSR.

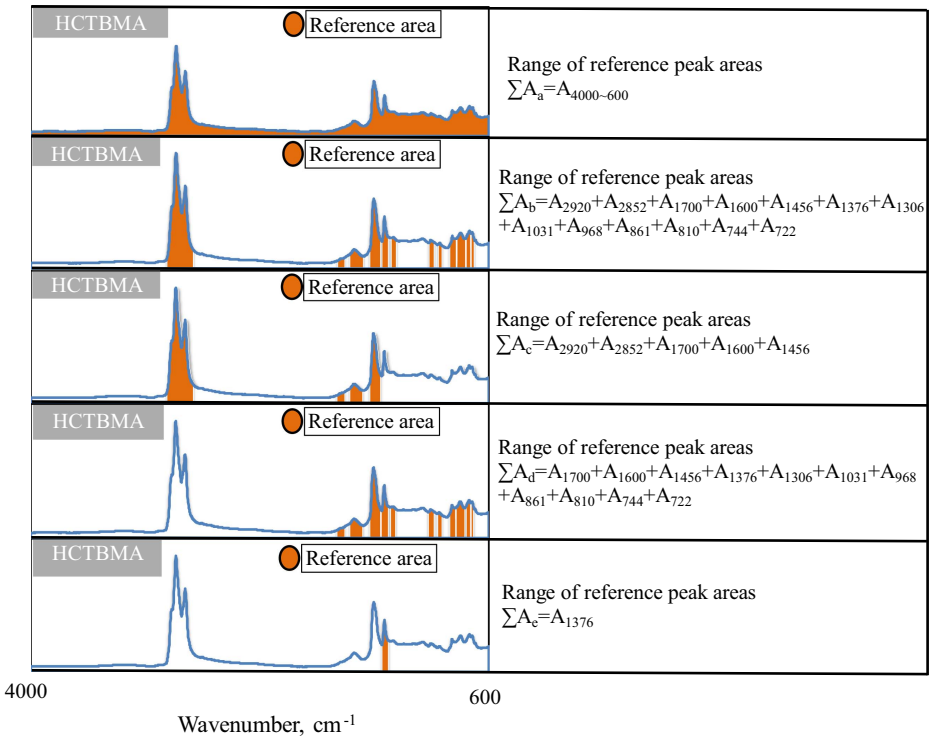

Fig. 1. Five infrared reference peak indexes used in the aging evaluation.

Table 2. I_{CA}, $I_{Si-O-Si}$, and I_{PB} calculation methods

Index	Calculation method
I_{CA}	$I_{CA} = A^{-1}_{1,700\ cm}/A^{-1}_{1,376\ cm}$
$I_{Si-O-Si}$	$I_{Si-O-Si} = A^{-1}_{1,100\ cm}/A^{-1}_{1,376\ cm}$
I_{PB}	$I_{PB} = A^{-1}_{966\ cm}/A^{-1}_{1376\ cm}$

Results and Discussion

ATR-FTIR Analysis

Fig. 2 shows the FTIR spectra of the RMA with different contents of CR and SBS before and after RTFOT and PAV. Fig. 3 shows the values of I_{PB}. ΔI_{CA}, and $\Delta I_{Si-O-Si}$ that are used to quantify the degree of oxidation and level of desulfurization of CR of RMA (Wang et al. 2020). The difference in I_{CA} between unaged and aged RMA is ΔI_{CA}, and $\Delta I_{Si-O-Si}$ is calculated in the same way as ΔI_{CA}. The ΔI_{CA} and $\Delta I_{Si-O-Si}$ values are listed in Tables 3 and 4. Under RTFOT and PAV, the I_{CA} of the RMA containing different contents of CR and SBS is lower than that of the Neat_E. Moreover, as described in Table 3, the ΔI_{CA} of the RMA containing different contents of CR and SBS after RTFOT and PAV aging is lower than that of the Neat_E, indicating that the degree of oxidation of RMA containing different contents of CR and SBS is lower than that of Neat_E. The 20TB_5SBS and 40TB_3SBS have the smallest ΔI_{CA} values under RTFOT and PAV, respectively. The ΔI_{CA} ranking is 20TB_5SBS < 20TB_3SBS < 40TB_5SBS < 40TB_3SBS < Neat_E after RTFOT and the ΔI_{CA}'s ranking is 40TB_3SBS < 20TB_3SBS = 40TB_5SBS < 20TB_5SBS < Neat_E after PAV aging. It is shown that increasing the SBS content can retard the oxidation of HCTBMA during RTFOT, but an increase in SBS content during PAV leads to a decrease in inhibiting the oxidation of HCTBMA. This is due to the higher silica index of 40TB_3SBS compared with 40TB_5SBS after PAV aging (as shown in Table 4), indicating a higher degree of desulfurization of 40TB_3SBS, which has a softening effect and inhibits the production of carbonyl groups, improving the resistance of 40TB_3SBS to PAV aging.

According to Table 4, the $I_{Si-O-Si}$ ranking is Neat_E = 0 < 20 TB_5SBS < 20 TB_3SBS < 40 TB_5SBS < 40 TB_3SBS before aging, indicating that compared with Neat_E, RMA containing different contents of CR and SBS has silica and as the CR in the RMA increases, the proportion of silica in the RMA also increases. The silica index of 20TB_3SBS is greater than that of 20TB_5SBS, and the silica index of 40TB_3SBS is greater than that of 40TB_5SBS. The reason is that after adding SBS to HCTBMA, the different content of SBS leads to a different degree of cross-linking reaction between SBS and HCTBMA, which influences the effect of silica release in CR flowing into HCTBMA. It also shows that the silica in CR is more easily released into HCTBMA when the SBS content in HCTBMA is relatively low (3%). Besides, from RTFOT to PAV aging, the $I_{Si-O-Si}$ increases for the same RMA, indicating that CR continues to carry out a desulfurization reaction with the aggravation of aging, resulting in the release of silica from CR to the bituminous phase. The $\Delta I_{Si-O-Si}$ ranking after RTFOT and PAV is 20TB_3SBS < 40TB_3SBS < 20TB_5SBS < 40TB_5SBS, indicating as SBS content increases, aging can aggravate the flow of silica in CR into asphalt phase. Meanwhile, as shown in Fig. 3, compared with the RMA containing different contents of CR and SBS, the I_{PB} of Neat_E is lower under unaged conditions and the I_{PB} ranking under unaged conditions is Neat_E < 20TB_3SBS < 20TB_5SBS < 40TB_3SBS < 40TB_5SBS, indicating that a higher content of CR and SBS leads to a higher content of polybutadiene polymer in RMA. The I_{PB} values of RMA containing different contents of CR and SBS increase and then decrease with aging due to the short-term aging of RMAs dominated by

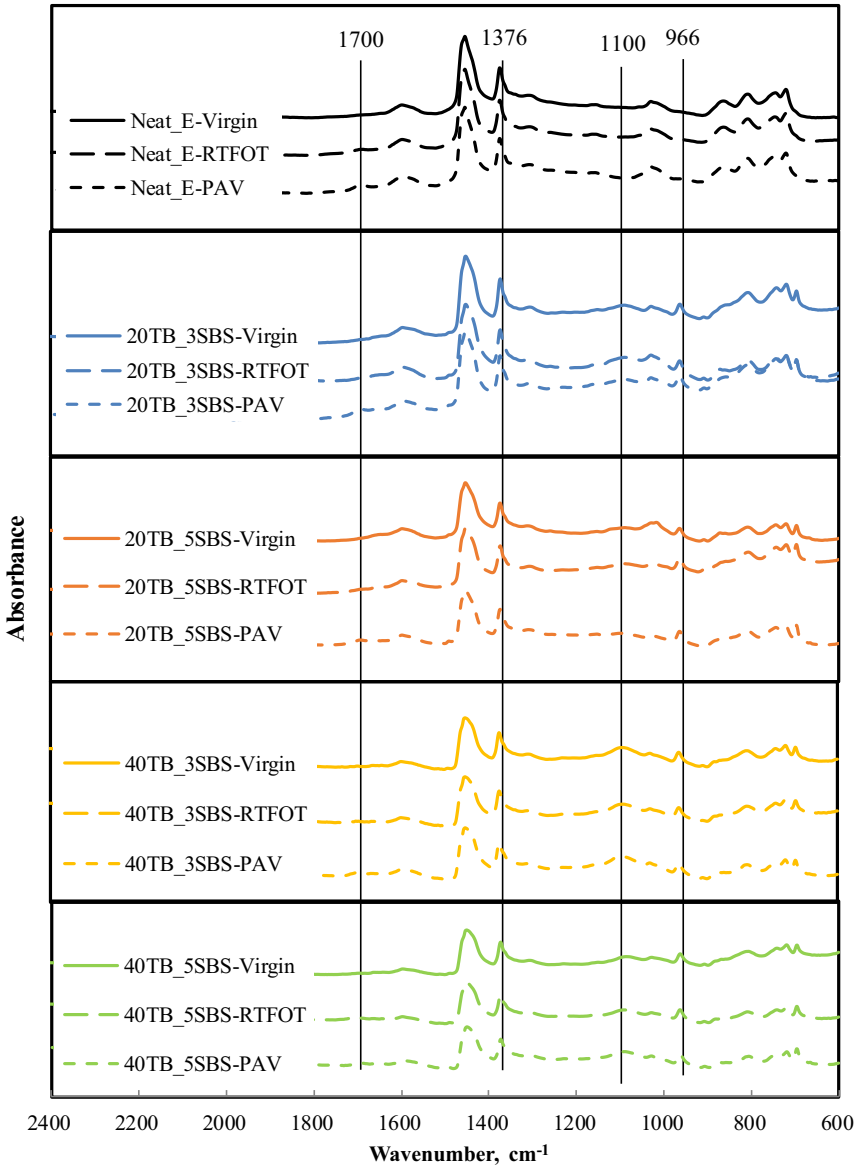

Fig. 2. ATR-FTIR spectra of RMA containing different contents of CR and SBS before and after aging.

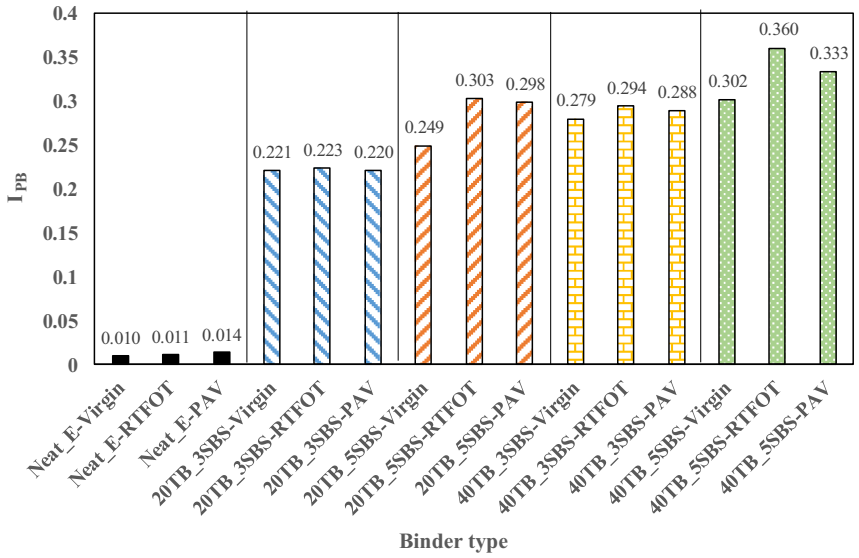

Fig. 3. I_{PB} of RMA containing different contents of CR and SBS.

Table 3. ΔI_{CA} of RMA containing different contents of CR and SBS before and after aging

	Neat_E		20TB_3SBS		20TB_5SBS		40TB_3SBS		40TB_5SBS	
Aging state	I_{CA}	ΔI_{CA}	I_{CA}	ΔI_{CA}	I_{CA}	ΔI_{CA}	I_{CA}	ΔI_{CA}	I_{CA}	ΔI_{CA}
Unaged	0.08	—	0.03	—	0.02	—	0.04	—	0.06	—
RTFOT aging	0.16	0.08	0.07	0.04	0.05	0.03	0.10	0.06	0.10	0.05
PAV aging	0.28	0.20	0.20	0.17	0.20	0.19	0.20	0.16	0.23	0.17

Table 4. $\Delta I_{Si-O-Si}$ of RMA containing different contents of CR and SBS before and after aging

	Neat_E		20TB_3SBS		20TB_5SBS		40TB_3SBS		40TB_5SBS	
Aging state	$I_{Si-O-Si}$	$\Delta I_{Si-O-Si}$	$I_{Si-O-Si}$	$\Delta I_{Si-O-Si}$	$I_{Si-O-Si}$	$\Delta I_{Si-O-Si}$	$I_{Si-O-Si}$	$\Delta I_{Si-O-Si}$	$I_{Si-O-Si}$	$\Delta I_{Si-O-Si}$
Unaged	0	0	0.300	—	0.185	—	0.664	—	0.458	—
RTFOT aging	0	0	0.309	0.009	0.234	0.049	0.702	0.038	0.627	0.169
PAV aging	0	0	0.334	0.034	0.256	0.070	0.721	0.057	0.650	0.192

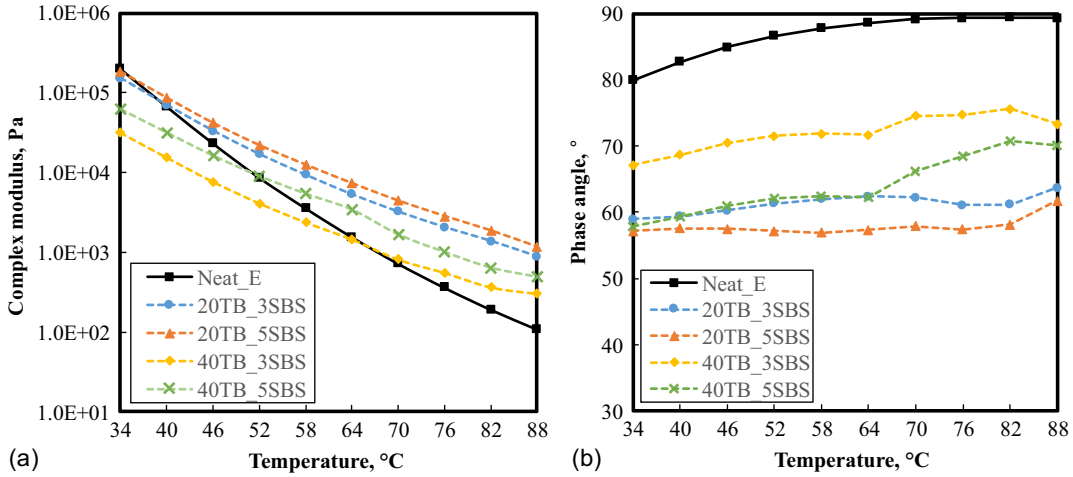

Fig. 4. (a) G^*; and (b) δ of RMA containing different contents of CR and SBS.

the desulfurization of CR and their long-term aging dominated by the degradation of polybutadiene (Wang et al. 2021b).

TS Test Result Analysis

Evaluation of G^* and δ before Aging

Fig. 4 shows the changes in G^* and δ of the RMA containing various CR and SBS contents. The G^* of Neat_E is higher than that of the other RMA at 34°C, indicating that compared with RMA, Neat_E has greater elasticity at 34°C. This may be because the CR in the RMA prepared by the TB process produces a desulfurization, causing it to lose rubber elasticity, resulting in a decrease in the elasticity of the RMA at 34°C (Han et al. 2016). When the temperature exceeds 70°C, the G^* ranking is Neat_E < 40TB_3SBS < 40TB_5SBS < 20TB_3SBS < 20TB_5SBS, indicating that the increase of CR content makes HCTBMA soft, which is because HCTBMA is prepared under high-temperature stirring conditions. In the TB process, the reticulated macromolecular structure in CR becomes a large number of small reticulated structures at high temperatures, thus obtaining partial plasticity, but also losing the elasticity of CR, and the higher the CR content, the more elasticity HCTBMA loses (Tang et al. 2016). The G^* value of Neat_E is smaller than that of the RMA containing different contents of CR and SBS. The δ ranking is the inverse of that of G^* at 76°C, which is 20TB_5SBS < 20TB_3SBS < 40TB_5SBS < 40TB_3SBS < Neat_E, indicating that adding the SBS in HCTBMA results in decreases of δ and increases of G^*, leading to an improvement in the elasticity of HCTBMA. The Neat_E's δ is higher than the RMA containing different contents of CR and SBS. The reason for this phenomenon is the rigid network structure formed by the polymers in SBS and CR in the RMA, which provides additional elasticity to the RMA.

Evaluation of G^* and δ after Aging

The G^* and δ of the RMA containing different contents of CR and SBS before and after aging are shown in Fig. 5. The G^* of the RMA containing different contents of CR and SBS before and after aging decreases gradually from 34°C to 88°C. Compared with the RMA containing different contents of CR and SBS, after RTFOT the increase of G^* of Neat_E is more obvious, indicating that the aging degree of the RMA containing different contents of CR and SBS after RTFOT is less serious than Neat_E. Compared with Neat_E, the increase of G^* of 20TB_5SBS, 40TB_3SBS, and 40TB_5SBS after PAV aging is less obvious, indicating that Neat_E has lower long-term aging resistance than HCTBMA. As described in Figs. 5(a and b), from RTFOT to PAV, the δ of Neat_E and 20TB_3SBS decreases gradually. Besides, based on Figs. 5(c–e),

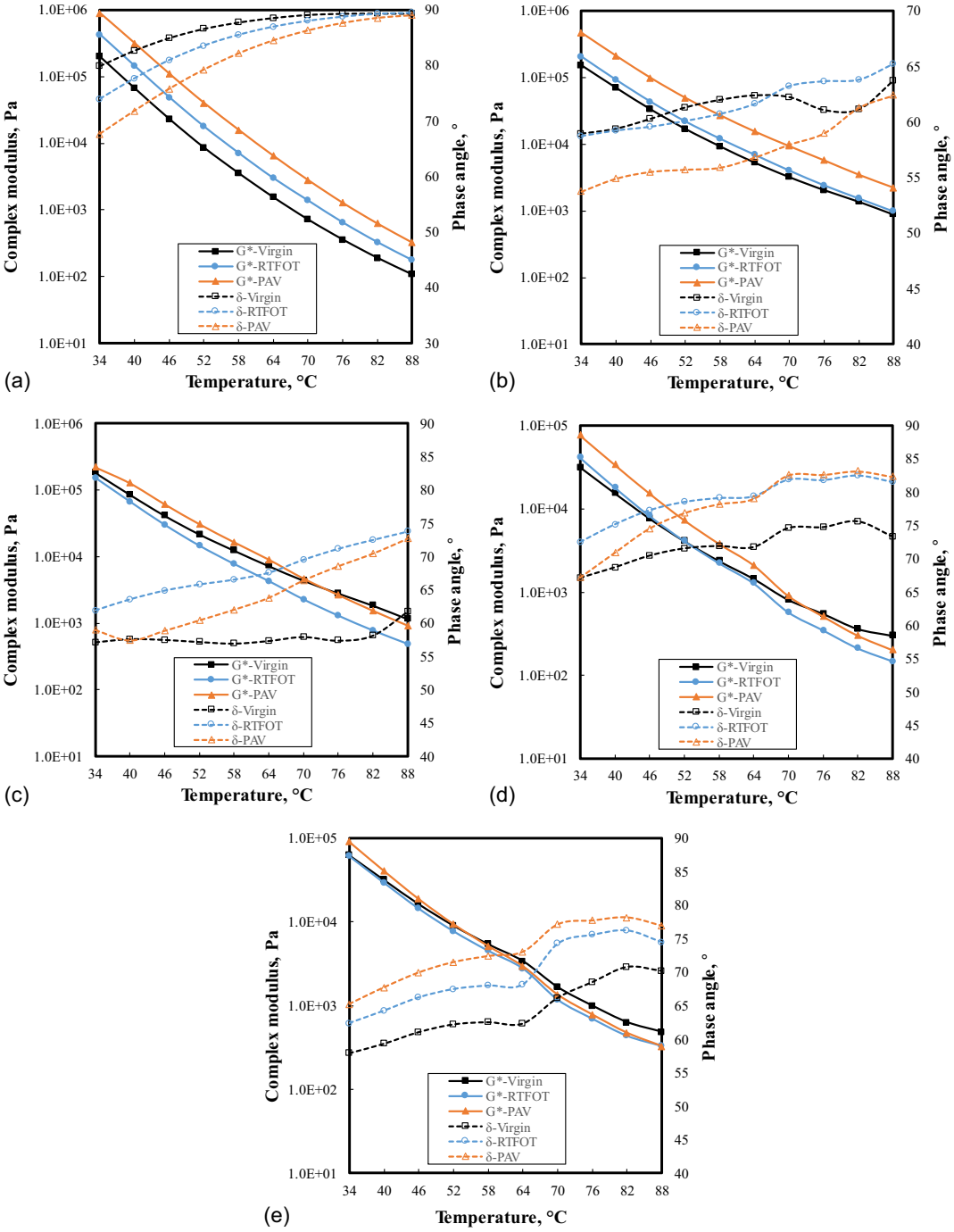

Fig. 5. G^* and δ of RMA containing different contents of CR and SBS after RTFOT and PAV: (a) Neat_E; (b) 20TB_3SBS; (c) 20TB_5SBS; (d) 40TB_3SBS; and (e) 40TB_5SBS.

the δ values of 20TB_5SBS, 40TB_3SBS, and 40TB_5SBS increase after aging. This phenomenon is because Neat_E hardens with aging, causing a drop in δ. In addition, aging degrades the SBS in HCTBMA, softening the asphalt and weakening the asphalt's hardening effect after aging, resulting in an increase in δ after aging in HCTBMA. Fig. 5 shows that the G^* and δ curves of the same HCTBMA in different aging states overlap at many temperatures. This is because the changes in the viscoelastic properties of HCTBMA during aging are jointly affected by the three processes of asphalt phase oxidation, CR desulfurization, and SBS degradation. The oxidation of the asphalt phase makes HCTBMA hard, leading to the increase of modulus and the decrease of δ. Additionally, CR desulfurization and SBS degradation cause damage to the polymer network, making HCTBMA soft, resulting in modulus reduction and δ increase. The three reactions occur simultaneously in the aging process. Therefore, when the G^* and δ curves of HCTBMA in different aging states coincide at the same temperature, it means that HCTBMA has the same viscoelastic properties after oxidation of the asphalt phase, CR desulfurization, and SBS degradation at this temperature.

Aging Resistance

The aging resistance of the RMA containing different contents of CR and SBS was assessed by the complex modulus aging index

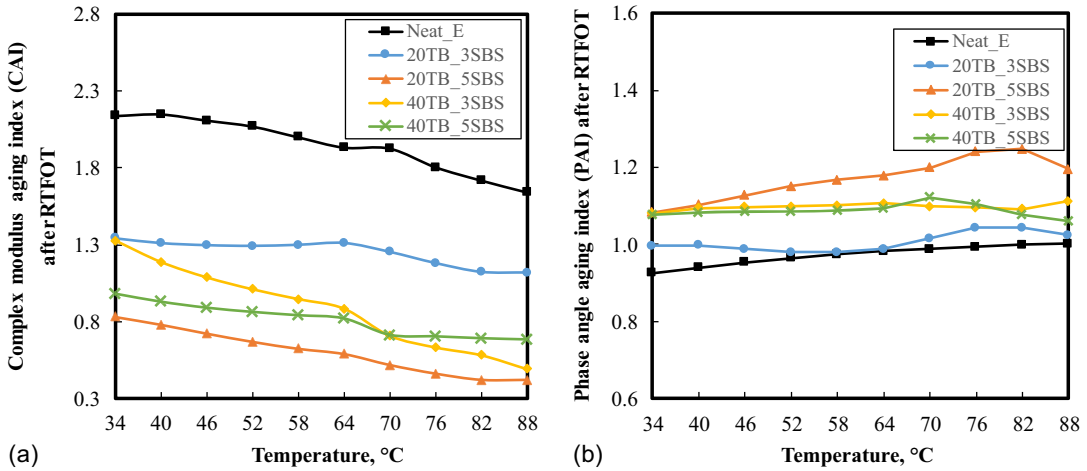

Fig. 6. (a) CAI; and (b) PAI of RMA containing different contents of CR and SBS after RTFOT.

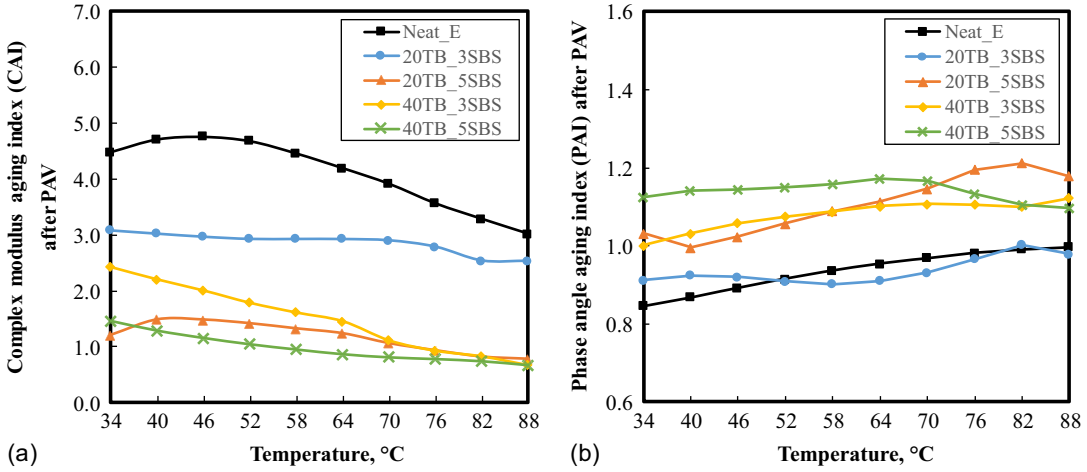

Fig. 7. (a) CAI; and (b) PAI of RMA containing different contents of CR and SBS after PAV.

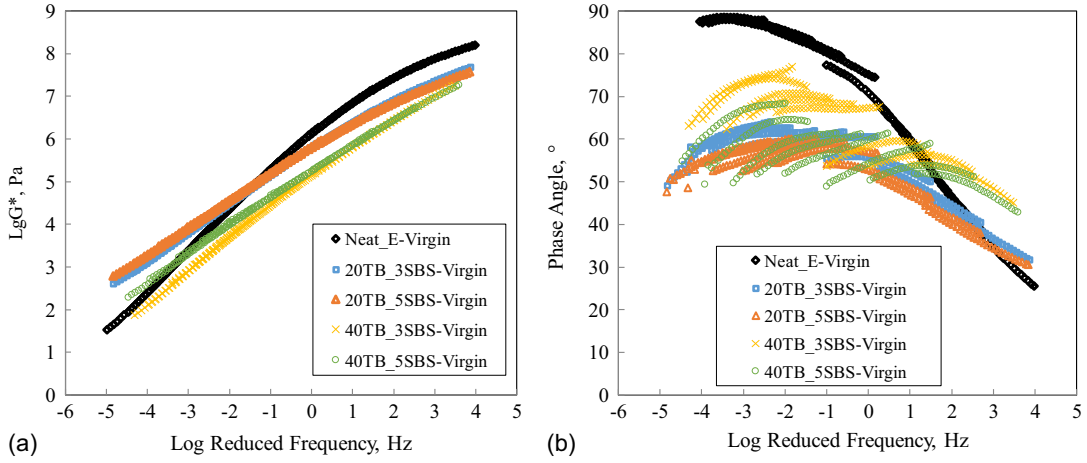

Fig. 8. Master curves of (a) G^*; and (b) δ of RMA containing different contents of CR and SBS.

(CAI) and phase angle aging index (PAI) (Wang et al. 2020, 2021a). The CAI is calculated from the ratio of the G^* after aging to the G^* before aging, and PAI is calculated in the same way as CAI. The bigger the CAI and the smaller the PAI, the worse the resistance to aging. Fig. 6 shows the CAI and PAI of the RMA containing different contents of CR and SBS after RTFOT aging, respectively. As described in Fig. 6(a), the CAI of the RMA containing different contents of CR and SBS is lower than that of

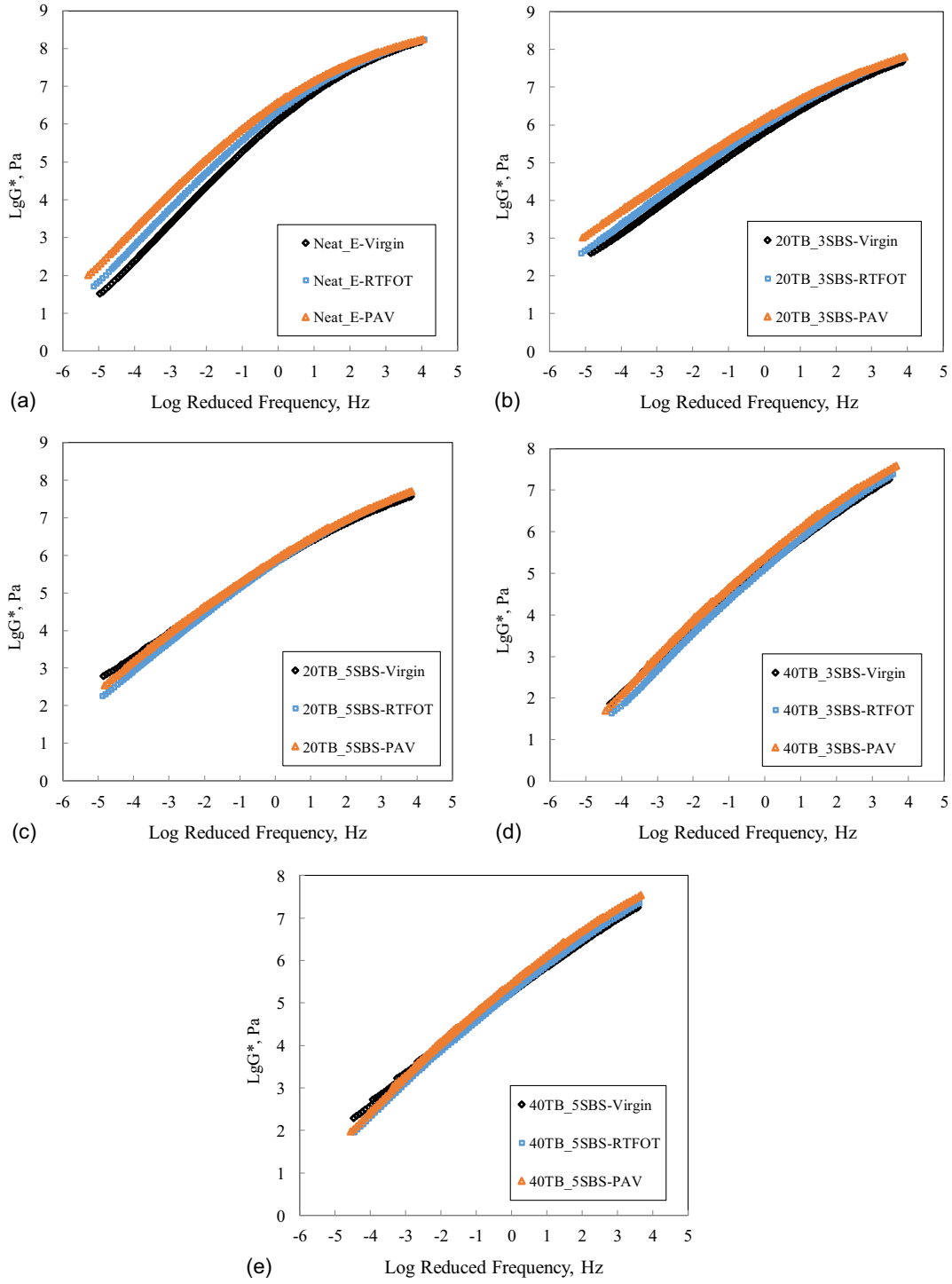

Fig. 9. G^* master curves of RMA containing different contents of CR and SBS after RTFOT and PAV: (a) Neat_E; (b) 20TB_3SBS; (c) 20TB_5SBS; (d) 40TB_3SBS; and (e) 40TB_5SBS.

Neat_E. In addition, the CAI ranking from 34°C to 70°C after RTFOT aging is 20TB_5SBS < 40TB_5SBS < 40TB_3SBS < 20TB_3SBS < Neat_E, and the CAI ranking from 70°C to 88°C after RTFOT aging is 20TB_5SBS < 40TB_3SBS < 40TB_5SBS < 20TB_3SBS < Neat_E. In Fig. 6(b), the PAI values of the RMA containing different contents of CR and SBS are higher than that of Neat_E, indicating that HCTBMA has better short-term anti-aging properties than Neat_E. This is due to the action of the antiaging agent and carbon black in HCTBMA, which improves the aging resistance of HCTBMA (Wang et al. 2020; Wang and Huang 2021).

Fig. 7 lists the CAI and PAI of the RMA containing different contents of CR and SBS after PAV aging. According to Fig. 7, the CAI of the RMA containing different contents of CR and SBS decreases significantly compared with Neat_E. The ranking of CAI is 40TB_5SBS < 20TB_5SBS < 40TB_3SBS < 20TB_3SBS < Neat_E after PAV. In addition, Neat_E shows the lowest PAI at 40°C, and the CAI of 40TB_5SBS is the lowest from 40°C to

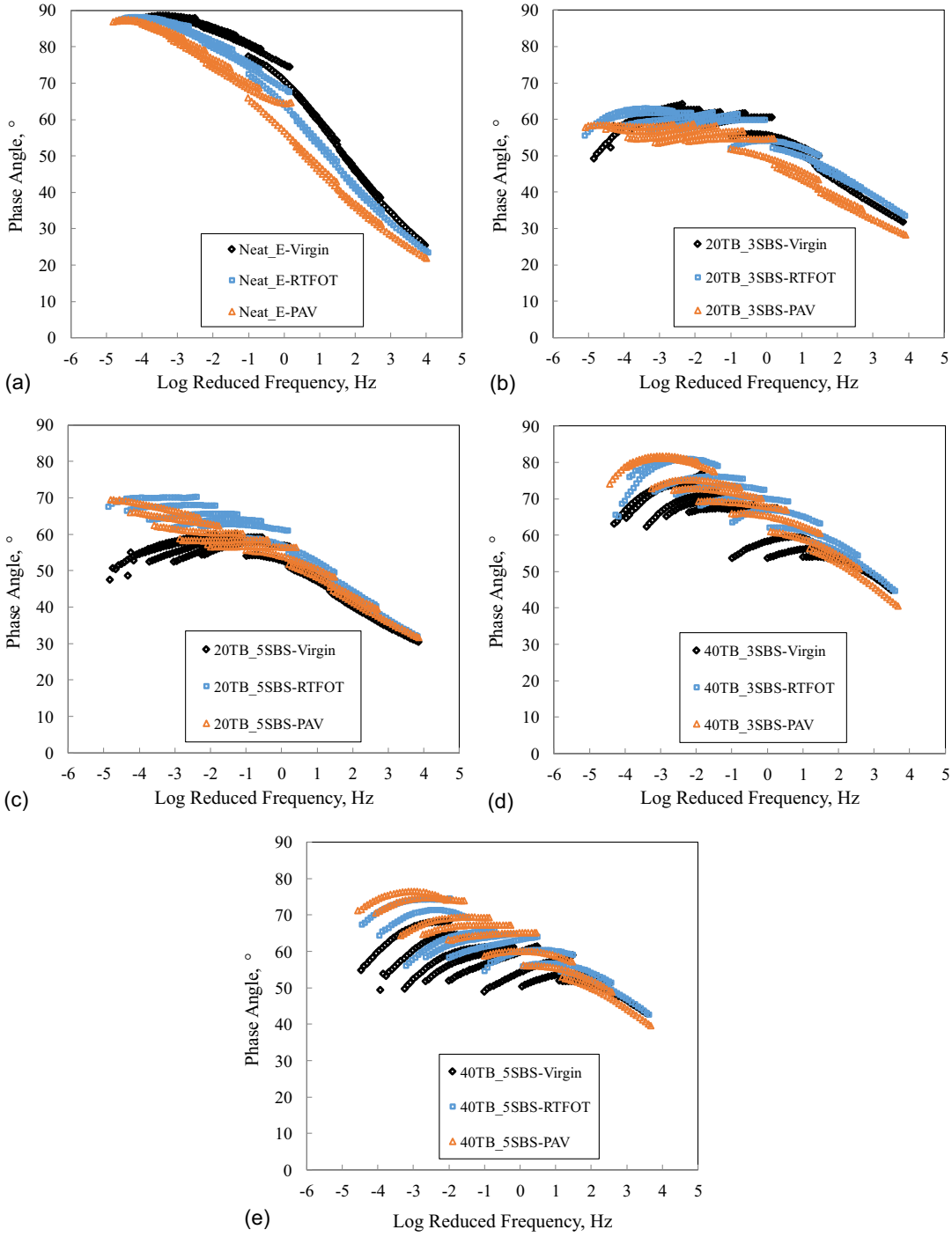

Fig. 10. δ master curves of RMA containing different contents of CR and SBS after RTFOT and PAV: (a) Neat_E; (b) 20TB_3SBS; (c) 20TB_5SBS; (d) 40TB_3SBS; and (e) 40TB_5SBS.

82°C, indicating SBS can enhance the long-term antiaging properties of HCTBMA. The reason for this phenomenon is that the degradation of SBS in HCTBMA reduces the age-hardening effect of HCTBMA.

Master Curves Result Analysis

Evaluation of Master Curves before Aging

Fig. 8 shows the master curves of G^* and δ of the RMA containing different contents of CR and SBS. As shown in Fig. 8(a), in the low-temperature region (high-frequency region), Neat_E has the largest G^* master curves, while Neat_E shows the lowest G^* master curves in the high-temperature region (low-frequency region). Furthermore, as shown in Fig. 8(b), the ranking of δ master curves of Neat_E and the RMA containing different contents of CR and SBS is similar to that of δ ranking in Fig. 4(b). These results show that compared with Neat_E, RMA containing different contents of CR and SBS has high elasticity at high temperatures. This is due to the addition of CR to the asphalt binder, forming a CR cross-linked structure. Carbon black plays the role of filling and reinforcement in CR, which can improve the strength of CR and effectively improve the elastic properties of RMA.

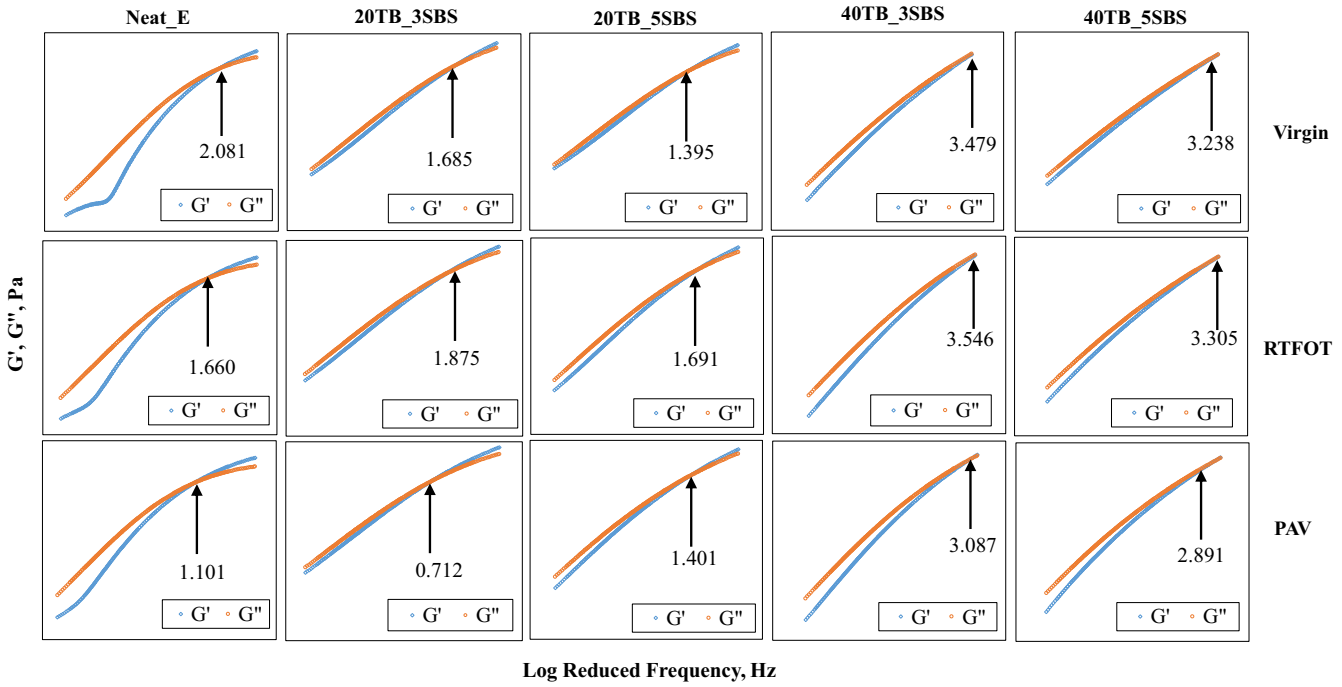

Fig. 11. Evolution of the master curves of G' and G'' of RMA containing different contents of CR and SBS with aging.

Evaluation of Master Curves after Aging

Figs. 9 and 10 show the master curves of G^* and δ of the RMA containing different contents of CR and SBS at various aging conditions. As shown in Figs. 9(a and b), the G^* master curves of Neat_E and 20TB_3SBS show an increasing trend with aging. Based on Figs. 9(c–e), aging has a small effect on the G^* master curves of 20TB_5SBS, 40TB_3SBS, and 40TB_5SBS. In other words, the G^* master curves of Neat_E and 20TB_3SBS increase significantly after aging compared with 20TB_5SBS, 40TB_3SBS, and 40TB_5SBS. From Fig. 10, with the aging degree deepening, the δ master curves of Neat_E present a monotonous downward trend in the full frequency range. This is because the neat asphalt does not contain a polymer phase, and the only asphalt phase has an enhanced elastic response after oxidation, driving the asphalt's δ down. The δ master curves of 20TB_5SBS, 40TB_3SBS, and 40TB_5SBS increase after aging. This indicates that the elasticity of 20TB_5SBS, 40TB_3SBS, and 40TB_5SBS decreases with aging, which is due to SBS degradation in 20TB_5SBS, 40TB_3SBS, and 40TB_5SBS.

The master curves of G' and G'' are sorted in terms of types of the RMA containing different contents of CR and SBS and presented in Fig. 11. With increasing frequency (lowering the temperature), the master curves of G' and G'' of the RMA containing different contents of CR and SBS increase. After aging, an increase in the logarithmic coordinates corresponding to the intersection point between the G' master curves and G'' master curves indicates softening of the asphalt. Table 5 displays the logarithmic coordinates corresponding to intersection points of the RMA containing different contents of CR and SBS. As shown in Table 5, the logarithmic coordinate corresponding to the intersection point of Neat_E decreases with more severe aging, indicating that the viscous components of Neat_E decrease with aging. The coordinates of the intersection point of the RMA containing different contents of CR and SBS increase and then decrease from the unaged state to the PAV state, implying that the elasticity of HCTBMA decreases and then increases after aging.

Table 5. Intersection points of RMA containing different contents of CR and SBS

	Logarithm of frequency corresponding to the intersection point (Hz)		
Sample	Virgin	RTFOT	PAV
Neat_E	2.081	1.66	1.101
20TB_3SBS	1.685	1.875	0.712
20TB_5SBS	1.395	1.691	1.401
40TB_3SBS	3.479	3.546	3.087
40TB_5SBS	3.238	3.305	2.891

MSCR Test Result Analysis

Evaluation of J_{nr} and R before Aging

Nonrecoverable creep compliance (J_{nr}) and recovery (R) were used as evaluation indexes to assess the rutting resistance of the RMA containing different contents of CR and SBS (D'Angelo 2009). The J_{nr} is denoted as $J_{nr0.1}$ and $J_{nr3.2}$ at two stress levels of 0.1 and 3.2 kPa, respectively, and $R_{0.1}$ and $R_{3.2}$ are defined in the same way. Based on Figs. 12 and 13, compared with the RMA containing different contents of CR and SBS, Neat_E has a higher $J_{nr0.1}$, and the ranking of $J_{nr3.2}$ is 20TB_5SBS < 20TB_3SBS < 40TB_5SBS < 40TB_3SBS < Neat_E. The rankings of $R_{0.1}$ and $R_{3.2}$ are Neat_E < 40TB_3SBS < 40TB_5SBS < 20TB_3SBS < 20TB_5SBS, illustrating that the rutting resistance of the RMA containing different contents of CR and SBS is better than that of Neat_E. Furthermore, the addition of SBS can enhance HCTBMA's rutting resistance. This indicates that the interaction between SBS and HCTBMA has an important effect on the final performance of the modified asphalt. The increase of SBS

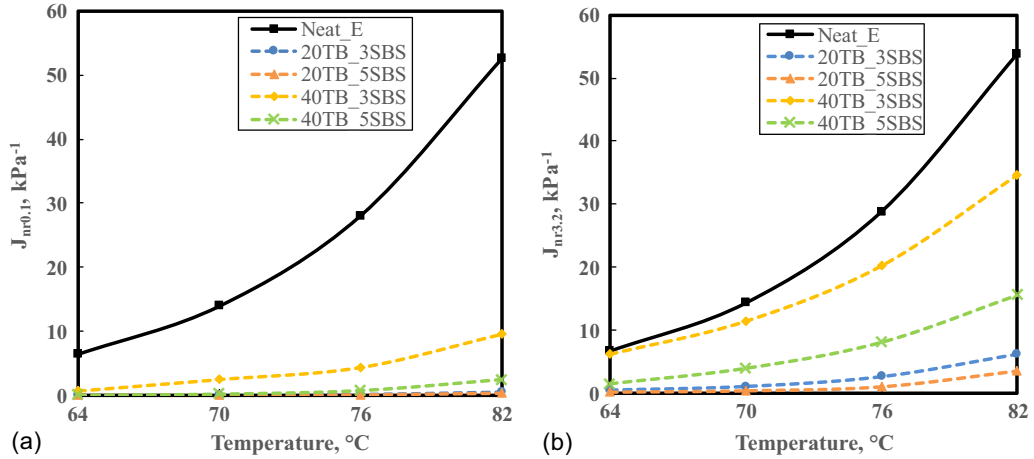

Fig. 12. J_{nr} of RMA containing different contents of CR and SBS: (a) $J_{nr0.1}$; and (b) $J_{nr3.2}$.

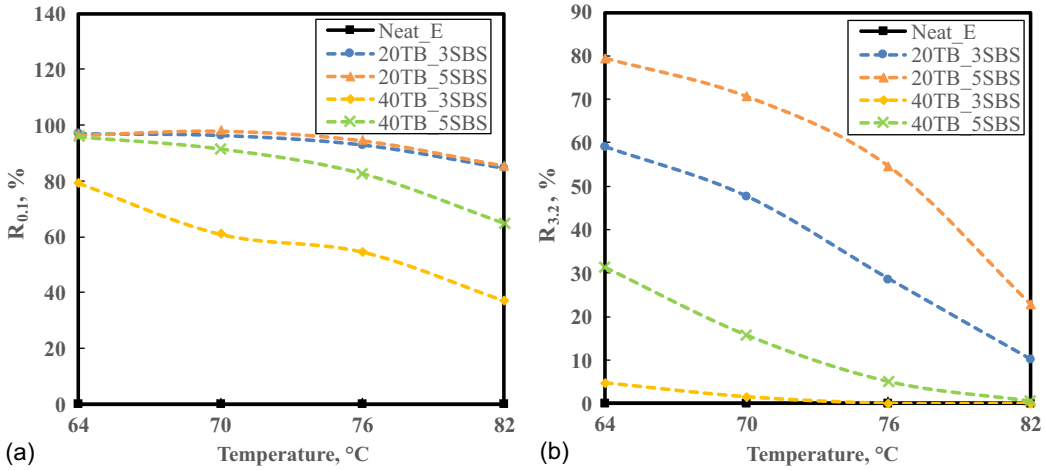

Fig. 13. R of RMA containing different contents of CR and SBS: (a) $R_{0.1}$; and (b) $R_{3.2}$.

admixture increased the number of elastic bodies in the asphalt, and the chemical reaction between SBS and CR formed a more complex continuous network structure, which had a positive effect on the significant improvement of the high-temperature rheological properties of SBS composite HCTBMA.

Evaluation of J_{nr} and R after Aging

The $J_{nr3.2}$ and $R_{3.2}$ indicators reflect changes in the viscoelastic properties of the asphalt. The smaller the value of $J_{nr3.2}$ and the larger the value of $R_{3.2}$, the more elastic the asphalt. Fig. 14 depicts the changes in $J_{nr3.2}$ of the RMA with different CR and SBS contents before and after aging. According to Fig. 14(a), the $J_{nr3.2}$ of Neat_E and 20TB_3SBS decreases gradually with more severe aging. This is due to the hardening and elasticity of the asphalt after aging. As described in Figs. 14(c–e), from RTFOT to PAV, the $J_{nr3.2}$ value of 20TB_5SBS, 40TB_3SBS, and 40TB_5SBS increases and then decreases. Fig. 15 shows the $R_{3.2}$ of the RMA containing different contents of CR and SBS before and after aging. The $R_{3.2}$ of the RMA containing different contents of CR and SBS is the opposite of the ranking of J_{nr}. From RTFOT to PAV, the $R_{3.2}$ of 20TB_3SBS, 20TB_5SBS, 40TB_3SBS, and 40TB_5SBS first decreases and then increases. This shows that the viscoelastic change of asphalt in $R_{3.2}$ after aging is consistent with that in $J_{nr3.2}$, and SBS degradation plays a leading role in the aging process, reducing the hardening degree of HCTBMA after aging. In Fig. 14, the overlap between the J_{nr} curves of unaged asphalt and the J_{nr} curves of aged asphalt is because the viscoelastic properties of HCTBMA after aging are the result of a game between three processes (desulfurization of CR, SBS phase degradation process, and asphalt phase hardening). The crossing of the unaged J_{nr} curve and the aged J_{nr} curve indicates that the viscoelastic properties of the unaged and aged HCTBMA are the same at this temperature.

Correlation Analysis

Pearson correlation analysis was performed in SPSS version 21 software to further investigate the relationship between chemical and rheological indexes of different contents of RMA prepared by the TB process. The P value represents the Pearson correlation coefficient, and the N value represents the number of samples. The Pearson correlation of chemical and rheological indexes of different contents of RMA prepared by the TB process are presented in Table 6. Here, $G^*_{70°C}$, $\delta_{70°C}$, $J_{nr0.1,70°C}$, $J_{nr3.2,70°C}$, $R_{0.1,70°C}$, and $R_{3.2,70°C}$ indicate these rheological indexes at 70°C. As shown in Table 6, it can be seen that the absolute value of the Pearson correlation coefficient between I_{PB} and $I_{Si-O-Si}$ is the largest ($|r| = 0.801$), followed by $R_{0.1,70°C}$ ($|r| = 0.670$), $J_{nr0.1,70°C}$ ($|r| = 0.578$), $\delta_{70°C}$ ($|r| = 0.510$), intersection points ($|r| = 0.238$),

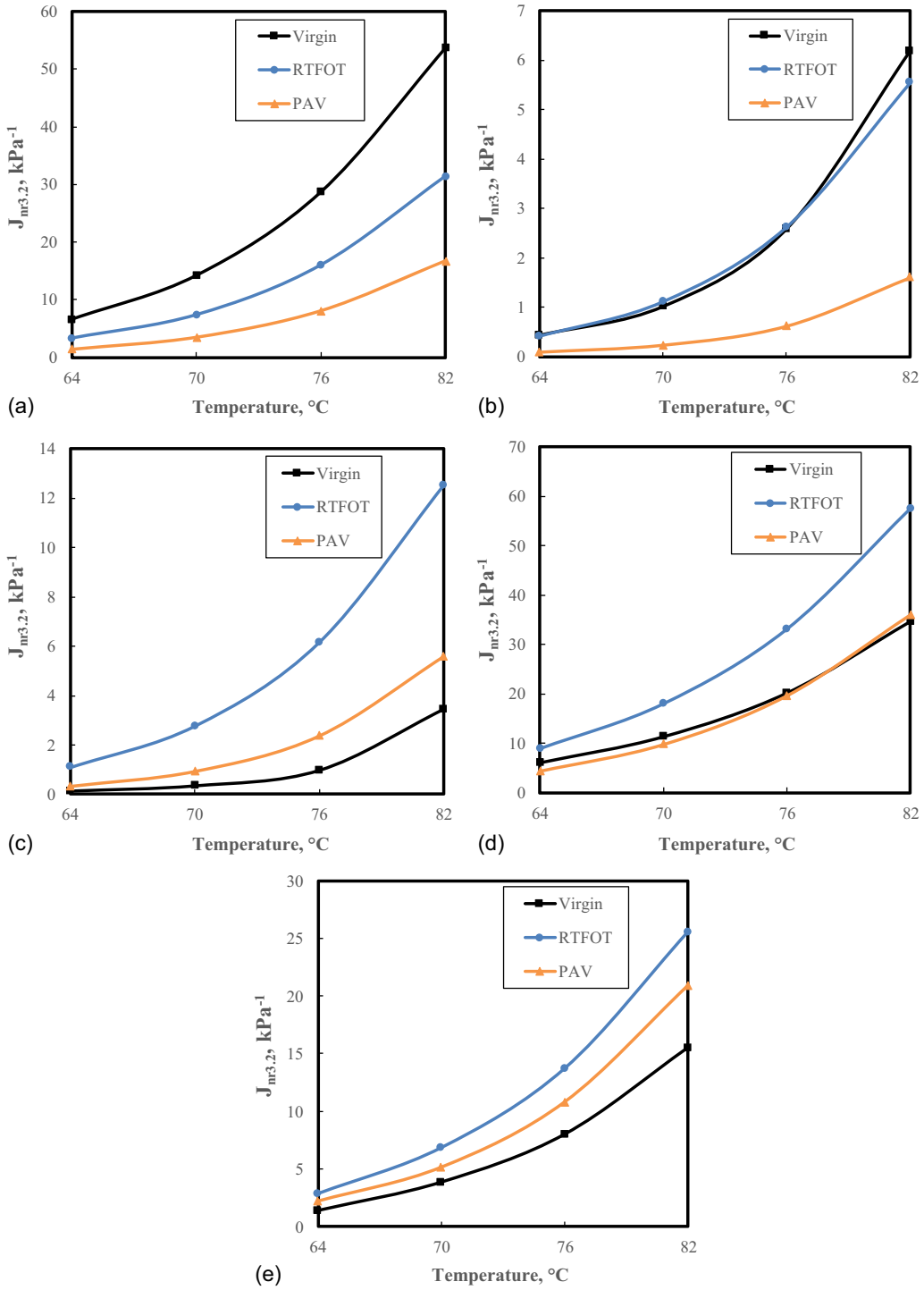

Fig. 14. $J_{nr3.2}$ of RMA containing different contents of CR and SBS after RTFOT and PAV: (a) Neat_E; (b) 20TB_3SBS; (c) 20TB_5SBS; (d) 40TB_3SBS; and (e) 40TB_5SBS.

I_{CA} ($|r| = 0.230$), $R_{3.2,70°C}$ ($|r| = 0.174$), $J_{nr3.2,70°C}$ ($|r| = 0.115$), and $G^*_{70°C}$ ($|r| = 0.001$), indicating that there is a good correlation between I_{PB} and $I_{Si-O-Si}$, and that the correlation between CR desulfurization and polybutadiene degradation in RMA prepared by the TB process during aging is high. However, the absolute value of the Pearson correlation coefficient between $G^*_{70°C}$ and $J_{nr0.1,70°C}$, $J_{nr3.2,70°C}$, and $R_{0.1,70°C}$ are 0.507, 0.704, and 0.501, respectively. These results indicate the correlation between $G^*_{70°C}$, $J_{nr0.1,70°C}$, $J_{nr3.2,70°C}$, and $R_{0.1,70°C}$ is not high, perhaps because the DSR oscillation test's indexes and MSCR test's indexes of different contents of RMA prepared by the TB process are not well correlated. Additionally, compared with the absolute value of the Pearson correlation coefficient between the DSR oscillation test's indexes and chemical indexes, the absolute value of the Pearson correlation coefficients between the MSCR test's indexes and chemical indexes are bigger, indicating the correlations between the MSCR test's indexes and chemical indexes are high.

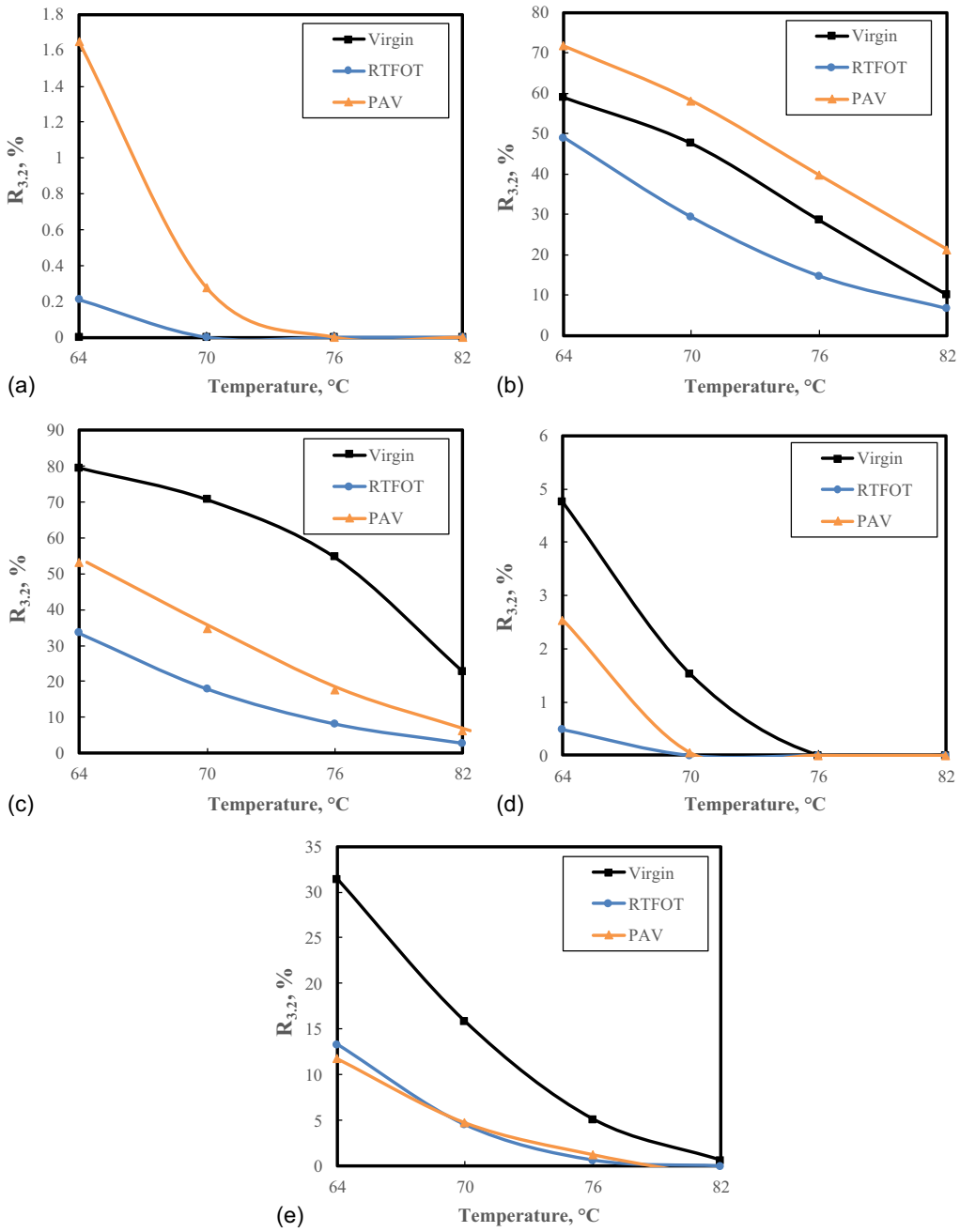

Fig. 15. $R_{3.2}$ of RMA containing different contents of CR and SBS after RTFOT and PAV: (a) Neat_E; (b) 20TB_3SBS; (c) 20TB_5SBS; (d) 40TB_3SBS; and (e) 40TB_5SBS.

Conclusion

In this research, the effect of SBS on the aging properties of different contents of RMA prepared by the TB process were investigated by chemo-rheological methods. The following are the main conclusions:

- ATR-FTIR observations show that SBS can retard the oxidation effect of HCTBMA during RTFOT, but the inhibitory effect of SBS during PAV is reduced. CR in HCTBMA continues to carry out desulfurization reactions with the aggravation of aging. In addition, SBS content can retard the oxidation of HCTBMA during RTFOT, but an increase in SBS content during PAV leads to a decrease in inhibiting the oxidation of HCTBMA. The I_{PB} and $I_{Si-O-Si}$ can be recommended as chemical indicators to judge the degree of desulfurization of HCTBMA.
- Compared with HCTBMA, Neat_E has low elasticity at high temperatures and high elasticity at low temperatures. The addition of SBS can enhance HCTBMA's rutting resistance, and the combination of SBS and HCTBMA is recommended to improve the high-temperature performance of the pavement.
- Compared with Neat_E, HCTBMA has better short-term and long-term aging resistance due to some carbon black and silica entering the asphalt during the aging degradation of CR and forming part of HCTBMA, which slows down the aging of HCTBMA to some extent.

Table 6. Pearson correlation analysis results index

Index type	Correlation index	I_{CA}	$I_{Si-O-Si}$	I_{PB}	$G^*_{70°C}$	$\delta_{70°C}$	Intersection points	$J_{nr0.1,70°C}$	$J_{nr3.2,70°C}$	$R_{0.1,70°C}$	$R_{3.2,70°C}$
I_{CA}	P	1	−0.055	−0.230	0.189	0.382	−0.224	0.050	−0.068	−0.428	−0.267
	N	15	15	15	15	15	15	15	15	15	15
$I_{Si-O-Si}$	P	−0.055	1	0.801	−0.286	−0.074	0.047	−0.201	0.344	0.266	−0.234
	N	15	15	15	15	15	15	15	15	15	15
I_{PB}	P	−0.230	0.801	1	0.001	−0.510	0.238	−0.578	−0.115	0.670	0.174
	N	15	15	15	15	15	15	15	15	15	15
$G^*_{70°C}$	P	0.189	−0.286	0.001	1	−0.701	0.100	−0.507	−0.704	0.501	0.806
	N	15	15	15	15	15	15	15	15	15	15
$\delta_{70°C}$	P	0.382	−0.074	−0.510	−0.701	1	−0.358	0.799	0.733	−0.949	−0.880
	N	15	15	15	15	15	15	15	15	15	15
Intersection points	P	−0.224	0.047	0.238	0.100	−0.358	1	−0.370	−0.307	0.454	0.215
	N	15	15	15	15	15	15	15	15	15	15
$J_{nr0.1,70°C}$	P	0.050	−0.201	−0.578	−0.507	0.799	−0.370	1	0.821	−0.840	−0.576
	N	15	15	15	15	15	15	15	15	15	15
$J_{nr3.2,70°C}$	P	−0.068	0.344	−0.115	−0.704	0.733	−0.307	0.821	1	−0.668	−0.722
	N	15	15	15	15	15	15	15	15	15	15
$R_{0.1,70°C}$	P	−0.428	0.266	0.670	0.501	−0.949	0.454	−0.840	−0.668	1	0.727
	N	15	15	15	15	15	15	15	15	15	15
$R_{3.2,70°C}$	P	−0.267	−0.234	0.174	0.806	−0.880	0.215	−0.576	−0.722	0.727	1
	N	15	15	15	15	15	15	15	15	15	15

Note: P = pearson correlation; and N = sample number.

- Pearson correlation analysis shows a strong correlation between CR desulfurization and polybutadiene degradation in RMA prepared by the TB process during aging. Additionally, compared with the DSR oscillation test's indexes, the correlations between the MSCR test's indexes and chemical indexes are high during aging.

Data Availability Statement

Some or all data, models, or code that support the findings of this study are available from the corresponding author upon reasonable request.

Acknowledgments

Thank you for financial support from the China Scholarship Council (CSC No. 202106260114).

References

AASHTO. 2014. *Standard specification for performance-graded asphalt binder using multiple stress creep recovery (MSCR) test*. AASHTO M 332-14. Washington, DC: AASHTO.

Abdelrahman, M. 2006. "Controlling performance of crumb rubber-modified binders through addition of polymer modifiers." *Transp. Res. Rec.* 1962 (1): 64–70. https://doi.org/10.1177/0361198106196200108.

Al-Mansob, R. A., et al. 2022. "Effect of carbon nanofibers on physical, adhesion and rheological properties of liquid epoxidized natural rubber modified asphalt." *Materials (Basel)* 15 (11): 3870. https://doi.org/10.3390/ma15113870.

Al-Sabaeei, A. M., A. Al-Fakih, S. Noura, E. Yaghoubi, W. Alaloul, R. A. Al-Mansob, M. Imran Khan, and N. S. Aliyu Yaro. 2022. "Utilization of palm oil and its by-products in bio-asphalt and bio-concrete mixtures: A review." *Constr. Build. Mater.* 337 (Jun): 127552. https://doi.org/10.1016/j.conbuildmat.2022.127552.

Apeagyei, A. K. 2011. "Laboratory evaluation of antioxidants for asphalt binders." *Constr. Build. Mater.* 25 (1): 47–53. https://doi.org/10.1016/j.conbuildmat.2010.06.058.

Arega, Z., A. Bhasin, A. Motamed, and F. Turner. 2011. "Influence of warm-mix additives and reduced aging on the rheology of asphalt binders with different natural wax contents." *J. Mater. Civ. Eng.* 23 (10): 1453–1459. https://doi.org/10.1061/(ASCE)MT.1943-5533.0000315.

Asli, H., E. Ahmadinia, M. Zargar, and M. R. Karim. 2012. "Investigation on physical properties of waste cooking oil—Rejuvenated bitumen binder." *Constr. Build. Mater.* 37 (Dec): 398–405. https://doi.org/10.1016/j.conbuildmat.2012.07.042.

Bressi, S., N. Fiorentini, J. Huang, and M. Losa. 2019. "Crumb rubber modifier in road asphalt pavements: State of the art and statistics." *Coatings* 9 (6): 384. https://doi.org/10.3390/coatings9060384.

D'Angelo, J. A. 2009. "The relationship of the MSCR test to rutting." Supplement, *Road Mater. Pavement Des.* 10 (S1): 61–80. https://doi.org/10.1080/14680629.2009.9690236.

Dong, R., J. Li, and S. Wang. 2011. "Laboratory evaluation of predevulcanized crumb rubber–modified asphalt as a binder in hot-mix asphalt." *J. Mater. Civ. Eng.* 23 (8): 1138–1144. https://doi.org/10.1061/(ASCE)MT.1943-5533.0000277.

Han, L., M. Zheng, and C. Wang. 2016. "Current status and development of terminal blend tyre rubber modified asphalt." *Constr. Build. Mater.* 128 (Dec): 399–409. https://doi.org/10.1016/j.conbuildmat.2016.10.080.

Jones, D., J. T. Harvey, and C. L. Monismith. 2008. *Reflective cracking study: Summary report*. Berkeley, CA: Univ. of California Pavement Research Center.

Li, M., L. Liu, C. Xing, L. Liu, and H. Wang. 2021. "Influence of rejuvenator preheating temperature and recycled mixture's curing time on performance of hot recycled mixtures." *Constr. Build. Mater.* 295 (Aug): 123616. https://doi.org/10.1016/j.conbuildmat.2021.123616.

Lin, P., W. Huang, N. Tang, and F. Xiao. 2017. "Performance characteristics of terminal blend rubberized asphalt with SBS and polyphosphoric acid." *Constr. Build. Mater.* 141 (6): 171–182. https://doi.org/10.1016/j.conbuildmat.2017.02.138.

Liu, L., M. Li, and Q. Lu. 2020. "Two-step mixing process elaboration of the hot-mix asphalt mixture based on surface energy theory." *J. Mater. Civ. Eng.* 32 (10): 04020301. https://doi.org/10.1061/(ASCE)MT.1943-5533.0003400.

Lo Presti, D. 2013. "Recycled tyre rubber modified bitumens for road asphalt mixtures: A literature review." *Constr. Build. Mater.* 49 (Dec): 863–881. https://doi.org/10.1016/j.conbuildmat.2013.09.007.

Lo Presti, D., G. Airey, and P. Partal. 2012. "Manufacturing terminal and field bitumen-tyre rubber blends: The importance of processing conditions." *Procedia-Social Behav. Sci.* 53 (Oct): 485–494. https://doi.org/10.1016/j.sbspro.2012.09.899.

Ministry of Transport of the People's Republic of China. 2011. *Standard test methods of bitumen and bituminous mixtures for highway engineering*. JTG E20-2011. Beijing: Ministry of Transport of the People's Republic of China.

Nazzal, M. D., M. T. Iqbal, S. S. Kim, A. Abbas, M. T. Quasema, and W. Mogawer. 2017. "Evaluating the mechanical properties of terminal blend tire rubber mixtures incorporating RAP." *Constr. Build. Mater.* 138 (May): 427–433. https://doi.org/10.1016/j.conbuildmat.2017.01.102.

Picado-Santos, L. G., S. D. Capitão, and J. M. C. Neves. 2020. "Crumb rubber asphalt mixtures: A literature review." *Constr. Build. Mater.* 247 (Jun): 118577. https://doi.org/10.1016/j.conbuildmat.2020.118577.

Qi, X., A. Shenoy, G. Al-Khateeb, T. Arnold, N. Gibson, J. Youtcheff, and T. Harman. 2006. "Laboratory characterization and full-scale accelerated performance testing of crumb rubber asphalts and other modified asphalt systems." In *Proc., Asphalt Rubber 2006 Conf.*, 39–65. Milton Park, UK: Taylor&Francis.

Safari, F., J. Lee, L. A. H. Do Nascimento, C. Hintz, and Y. R. Kim. 2014. "Implications of warm-mix asphalt on long term oxidative aging and fatigue performance of asphalt binders and mixtures." *Asphalt Paving Technol.* 83 (Jan): 143–169.

Santucci, L. 2009. "Rubber roads: Waste tires find a home." *Pavement Technol. Update* 1 (2): 1–12.

Shen, J., B. Li, and Z. Xie. 2017. "Interaction between crumb rubber modifier (CRM) and asphalt binder in dry process." *Constr. Build. Mater.* 149 (Jul): 202–206. https://doi.org/10.1016/j.conbuildmat.2017.04.191.

Sienkiewicz, M., K. Borzędowska-Labuda, A. Wojtkiewicz, and H. Janik. 2017. "Development of methods improving storage stability of bitumen modified with ground tire rubber: A review." *Fuel Process. Technol.* 159 (May): 272–279. https://doi.org/10.1016/j.fuproc.2017.01.049.

Stimilli, A., G. Ferrotti, C. Conti, G. Tosi, and F. Canestrari. 2014. "Chemical and rheological analysis of modified bitumens blended with 'artificial reclaimed bitumen.'" *Constr. Build. Mater.* 63 (Jul): 1–10. https://doi.org/10.1016/j.conbuildmat.2014.03.047.

Tang, N., W. Huang, J. Hu, and F. Xiao. 2018. "Rheological characterisation of terminal blend rubberised asphalt binder containing polymeric additive and sulphur." *Road Mater. Pavement Des.* 19 (6): 1288–1300. https://doi.org/10.1080/14680629.2017.1305436.

Tang, N., W. Huang, and F. Xiao. 2016. "Chemical and rheological investigation of high-cured crumb rubber-modified asphalt." *Constr. Build. Mater.* 123 (Oct): 847–854. https://doi.org/10.1016/j.conbuildmat.2016.07.131.

Wang, H., Z. You, J. Mills-Beale, and P. Hao. 2012. "Laboratory evaluation on high temperature viscosity and low temperature stiffness of asphalt binder with high percent scrap tire rubber." *Constr. Build. Mater.* 26 (1): 583–590. https://doi.org/10.1016/j.conbuildmat.2011.06.061.

Wang, S., and W. Huang. 2021. "Investigation of aging behavior of terminal blend rubberized asphalt with SBS polymer." *Constr. Build. Mater.* 267 (1): 120870. https://doi.org/10.1016/j.conbuildmat.2020.120870.

Wang, S., W. Huang, and A. Kang. 2021a. "Evaluation of aging characteristics of high-viscosity asphalt: Rheological properties, rutting resistance, temperature sensitivity, homogeneity, and chemical composition." *J. Mater. Civ. Eng.* 33 (7): 04021149. https://doi.org/10.1061/(ASCE)MT.1943-5533.0003777.

Wang, S., W. Huang, and A. Kang. 2021b. "Laboratory evaluation of the properties of high-cured crumb rubber modified asphalt containing sulfur and polymer after the oxidative aging procedure." *Constr. Build. Mater.* 304 (8): 124611. https://doi.org/10.1016/j.conbuildmat.2021.124611.

Wang, S., W. Huang, and P. Lin. 2022a. "Low-temperature and fatigue characteristics of degraded crumb rubber–modified bitumen before and after aging." *J. Mater. Civ. Eng.* 34 (3): 04021493. https://doi.org/10.1061/(ASCE)MT.1943-5533.0004131.

Wang, S., W. Huang, P. Lin, Z. Wu, C. Kou, and B. Wu. 2021c. "Chemical, physical, and rheological evaluation of aging behaviors of terminal blend rubberized asphalt binder." *J. Mater. Civ. Eng.* 33 (11): 04021302. https://doi.org/10.1061/(ASCE)MT.1943-5533.0003931.

Wang, S., W. Huang, X. Liu, and P. Lin. 2022b. "Influence of high content crumb rubber and different preparation methods on properties of asphalt under different aging conditions: Chemical properties, rheological properties, and fatigue performance." *Constr. Build. Mater.* 327 (4): 126937. https://doi.org/10.1016/j.conbuildmat.2022.126937.

Wang, S., W. Huang, Q. Lv, C. Yan, P. Lin, and M. Zheng. 2020. "Influence of different high viscosity modifiers on the aging behaviors of SBSMA." *Constr. Build. Mater.* 253 (8): 119214. https://doi.org/10.1016/j.conbuildmat.2020.119214.

Wang, T., F. Xiao, S. Amirkhanian, W. Huang, and M. Zheng. 2017. "A review on low temperature performances of rubberized asphalt materials." *Constr. Build. Mater.* 145 (Aug): 483–505. https://doi.org/10.1016/j.conbuildmat.2017.04.031.

Xing, C., W. Jiang, M. Li, M. Wang, J. Xiao, and Z. Xu. 2022. "Application of atomic force microscopy in bitumen materials at the nanoscale: A review." *Constr. Build. Mater.* 342 (Aug): 128059. https://doi.org/10.1016/j.conbuildmat.2022.128059.